Deliverable D1.6 Report on downscaling global climate projections for catchment-scale hydrological modelling

Document authors:	Alexandre Devers, Claire Lauvernet, Jean-Philippe Vidal (INRAE)
Document contributors:	Louise Mimeau (INRAE), Annika Künne (FSU), Flora Branger (INRAE), Sven Kralisch (FSU), Thibault Datry (INRAE)

Abstract

Intermittent rivers and ephemeral streams (IRES) account for more than half of the world's rivers. However, few studies have investigated the evolution of IRES under climate change. Aiming to overcome this problem, DRYvER proposed to provide daily hydrological projections, daily flow conditions and flow intermittence indicators in 6 European Drying River Networks (DRNs).

The current work aims to produce reach-scale daily hydrological projections available for the period 1985-2100 for each DRN. To this end, coarse spatial resolution daily projections from Global Climate Models (GCMs) are downscaled to obtain high resolution projections over the period 1971-2100. Secondly, the high-resolution projections are used as input to the JAMS/J2000 model to obtain daily catchment-scale hydrological projections. Several GCMs are used as well as 3 shared socio-economic pathways (SSPs) to capture the uncertainty due to climate modelling and greenhouse gas emission scenarios.

The results show that the methodology is able to reproduce the historical hydrological behaviour of the DRNs in terms of seasonality, with some difficulties in Morava and Vantaanjoki regarding summer discharge. Regarding the future periods, the responses of the six catchments were clearly different, showing an impact of climate change closely related to their location. Spring, summer and autumn discharges show a decrease for all catchments and all SSPs considered. For winter discharge, two of the catchments show a slight increase, but the other four also show a decrease of varying intensity.

Keywords: hydrological projections, climate change, downscaling, CMIP6

Information Table

PROJECT INFORMATION	
PROJECT ID	**869226**
PROJECT FULL TITLE	**Securing biodiversity, functional integrity and ecosystem services in DRYing riVER networks**
PROJECT ACRONYM	**DRYvER**
FUNDING SCHEME	**Horizon Europe**
START DATE OF THE PROJECT	**1st September 2020**
DURATION	**48 months**
CALL IDENTIFIER	**LC-CLA-06-2019**

DELIVERABLE INFORMATION	
DELIVERABLE No AND TITLE	D1.6 Report on downscaling global climate projections for catchment-scale hydrological modelling
TYPE OF DELIVERABLE [1]	R
DISSEMINATION LEVEL [2]	PU
BENEFICIARY NUMBER AND NAME	1 - INRAE
AUTHORS	Alexandre Devers, Claire Lauvernet, Jean-Philippe Vidal
CONTRIBUTORS	Louise Mimeau, Annika Künne, Flora Branger, Sven Kralisch, Thibault Datry
WORK PACKAGE No	1
WORK PACKAGE LEADER WP LEADER VALIDATION DATE	Jean-Philippe Vidal 10 october 2023
COORDINATOR VALIDATION DATE	Thibault Datry

[1] **Use one of the following codes:**

R=Document, report (excluding the periodic and final reports)
DEM=Demonstrator, pilot, prototype, plan designs
DEC=Websites, patents filing,press & media actions, videos, etc.
OTHER=Software, technical diagram, etc.
ORDP : Open Research Data Pilot

[2] **Use one of the following codes:**

PU=Public, fully open, e.g. web
CO=Confidential, restricted under conditions set out in Model Grant Agreement
CI=Classified, information as referred to in Commission Decision 2001/844/EC.

Table of contents

1 Introduction

1.1 Background

Currently, more than half of the world's river channels are classified as intermittent rivers and ephemeral streams (IRES), which periodically stop flowing (Messager et al., 2021). Although IRES can occur naturally in any river network, they can be modified in space and time, mainly due to human water use and climate change. Indeed, global warming is predicted to have a strong impact on the hydrological cycle and hence on IRES, resulting in changes in wet and dry events and seasons (Arias et al., 2021). DRYvER's multi-model approach aims to simulate hydrological, biological and biogeochemical processes to assess biodiversity, ecosystem functions and services (Datry et al., 2021).

1.2 Objectives

The objective of Task 1.1 is to provide flow intermittence patterns for the six EU focal Drying River Networks (DRNs), for present conditions and future climate scenarios, taking into account human influences (e.g. abstraction, reservoirs) on hydrological process dynamics of the DRNs.

The current work aims at producing hydrological projections over the 1985-2100 period (T1.3). To that end, coarse spatial resolution daily projections from global climate models (GCMs) are downscaled to obtain high-resolution projections over the period 1971-2100. Secondly, the high-resolution projections are used as input to the JAMS/J2000 (see report D1.2) model to obtain daily reach-scale hydrological projections over the 6 catchments.

A step further was originally planned to constrain the reach-scale projections with output from global hydrological models, i.e. available at 0.5° resolution, through data assimilation. However, given the already high quality of discharge projections obtained through the combination of the downscaling step and the hydrological modeling step, this part of the task was abandoned. The report title has been modified accordingly.

2 Data and Method

2.1 Data

The following section describes the various sources of meteorological variables used to produce the downscaled climate projections.

2.1.1 High-resolution reanalysis

The ERA5-Land reanalysis (Muñoz-Sabater et al., 2021) provides hourly values of several surface meteorological variables at a resolution of 0.1° over the entire planet. It has been produced by replacing the land component of the ECMWF ERA5 climate reanalysis. Data are available from 1950 to the present and are updated monthly with a lag of about three months (Copernicus Climate Change Service (C3S) Climate Data Store (CDS), 2023).

For this study, hourly values of ERA5-Land were extracted over the six case study catchments between 1950-01-01 and 2021-12-31. The number of extracted cells varies with the catchment size: 66 for Ain, 33 for Fekete, 30 for Guadiaro, 33 for Krka, 155 for Morava and 45 for Vantaanjoki.

The following variables were extracted at the hourly time step and aggregated at the daily time step:

- 2m air temperature (° C),
- 2m dew point temperature (° C),
- 2m relative humidity (%)
- 10m u and v wind speed components (m/s),
- surface pressure (Pa).

Other variables are directly extracted at the end of the day:

- incoming solar radiation (W/m^2),
- incoming thermal radiation (W/m^2),
- total precipitation (mm).

Daily variables are then used to compute the reference evapotranspiration using the Penman-Monteith equation (Allen et al., 1998). For this study, only daily precipitation, temperature and evapotranspiration originating from the ERA5-Land have been used.

2.1.2 Coarse resolution global climate reanalysis

The W5E5 V2.0 dataset (Lange, 2019a) has been compiled to support the bias adjustment of climate input data for the impact assessments carried out in Phase 3 of the Inter-Sectoral Impact Model Intercomparison Project Phase 3 (ISIMIP3, www.isimip.org/, Frieler et al., 2023). It is based on the WATCH Forcing Data methodology (see Cucchi et al., 2020, for details) applied to surface meteorological variables from the ERA5 reanalysis (Hersbach et al., 2020) over land and the ERA5 reanalysis over the ocean. Over land, three steps were used to generate the dataset, which can be summarised as follows: (1) the ERA5 reanalysis was regridded to a regular half-degree longitude-latitude grid, (2) an elevation correction was applied as well as a bias correction based on the CRU TS (Harris et al., 2020) and GPCC datasets (Schneider et al., 2020), (3) the data were regridded at 0.5°.

The dataset is available on a daily basis between 1979-2019 and provides several meteorological variables. As for ERA5-Land, the 2m air temperature, 2m dew point temperature, 2m relative humidity, 10m u and v wind speed components, surface pressure, incoming solar radiation and incoming thermal radiation were used to calculate the reference evapotranspiration using the Penman-Monteith equation. Only the daily precipitation, temperature and evapotranspiration values from the W5E5 V2.0 data set will be used for the study.

2.1.3 Coarse resolution global climate projections

The climate projections from ISIMIP phases 3a -- for the period 1971-2014 (Frieler et al., 2023) -- and 3b -- for the period 2014-2100 -- are available on the website www.isimip.org/.

The projections consist of five CMIP6 (Eyring et al., 2016) GCMs selected on the basis of their historical performance and to reflect the climate sensitivity of the full CMIP6 ensemble (Shiogama et al., 2021). The CMIP6 GCMs were bias-adjusted to the W5E5 V2.0 dataset (Lange, 2019a) using a quantile mapping approach that preserves trends in all quantiles of the distribution of simulated daily climate model outputs (Lange, 2019b).

In our study we used the five GCMs (GFDL-ESM4 / IPSL-CM6A-LR / MPI-ESM1-2-HR / MRI-ESM2-0 / UKESM1-0-LL) and the three SSPs (sustainability [SSP1-2.6], regional rivalry [SSP3-7.0] and fossil-fuelled development [SSP5-8.5]) available in ISIMIP 3b.

Data are extracted at a daily time step between 1971 and 2100. As for the other meteorological datasets, the Penman-Monteith reference evapotranspiration is calculated using 2m air temperature, 2m dew point temperature, 2m relative humidity, 10m u and v wind speed components, surface pressure, incoming solar radiation and incoming thermal radiation. Finally, only daily precipitation, temperature and evapotranspiration from the global climate projection dataset are used. For clarity, the data will be referred to as PROJ in the remaining text.

2.2 Method

2.2.1 Climate downscaling

The first part of the methods section is dedicated to the presentation of the analogy method proposed to obtain high-resolution projections. The method is based on the hypothesis that similar coarse scale situations lead to similar high resolution situations (Lorenz, 1974). Globally, for future projections, high-resolution values are estimated through the selection of an analog day from an high-resolution historical archive – gridded observation or reanalysis – based on the values at coarse resolution. This type of methodology as been applied in various context to produced high-resolution climate projections.

Step 1:

The first step is to compute the daily mean catchment values of each of the meteorological variables, i.e. precipitation (P), temperature (T) and evapotranspiration (ET0). Considering the different products, the calculation is applied over different time periods:

- ERA5-Land: 1950-01-01 to 2021-12-31,
- W5E5: 1985-01-01 to 2014-12-31,
- PROJ: 1971-01-01 to 2100-12-31.

It should be noted that for each GCM and SSP, PROJ's catchment-average values are computed separately.

Step 2:

To account for the difference in spatial resolution between the PROJ outputs and the ERA5-Land reanalysis, a monthly correction is applied. The correction is based on the difference – for T – and ratio – for P and ET0 – between the mean monthly catchment values computed using ERA5-Land and W5E5 over the period 1985-2014. Figure 1 illustrates the seasonality of the correction. For the evapotranspiration, values are lower in ERA5-Land than in W5E5 over the winter period. Concerning the precipitation, the factors are between 0.9 and 1.1 – differences between -/+ 10% – for all catchments and all months except for July and August for Guadiaro. This strong difference is explained by the low amount of precipitation leading to high values in terms of percentage. Finally, for temperatures, the corrections are globally similar for all catchments, except for the Ain, with a higher temperature during the summer months in W5E5 than in ERA5-Land.

Figure 1

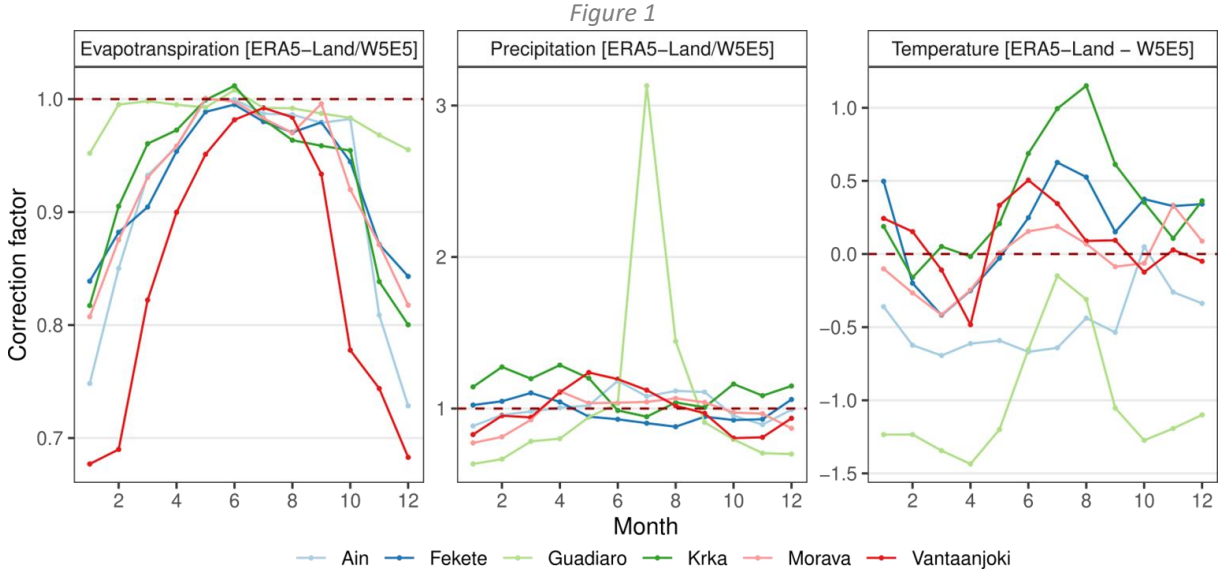

:Ratios (P and ET0) and differences (T) between mean monthly catchment values computed using W5E5 and ERA5-Land over 1985-2014.

The monthly correction factors are then applied to the daily mean catchment values from PROJ over the period 1971-2100. Note that the aim of the correction is to represent the difference of resolution between ERA5-Land and PROJ. This is not a bias correction, as PROJ are not corrected by factors derived from the direct comparison of ERA5-Land and PROJ. Furthermore, as the factors are calculated using W5E5, it is possible that applying this correction to PROJ may lead to a stronger bias in the meteorological variables.

Step 3:

Due to the large difference in climate between the historical period and the end of the century - especially for SSP3-7.0 and SSP5-8.5 - similar meteorological values could be difficult to find in the historical archive. Therefore, for both temperature and evapotranspiration, it was decided to remove linear trends before computing the anomalies and reapplying the trends afterwards (Clemins et al., 2019). The trends are calculated on the mean catchment values for each period, each variable and each month - and each GCM and each SSP for PROJ - allowing some flexibility in detrending.

The trends are removed:

- on ERA5-Land over 1950-2021 based on the 1985-2014 trends,
- on PROJ over 1971-2014 based on the 1985-2014 trends and over 2015-2100 based on the 2015-2100 trends.

Step 4:

Before comparing the catchment mean meteorological values, all products are transformed into anomalies according to the following formula:

$$A_{var} = (V_{var} - \overline{V_{var}}[m])/\sigma\,(V_{var}[m]) \qquad \text{(Eq. 1)}$$

where A_{var} are the daily anomalies and $_{var}$ the variable considered (i.e. T, P or ET0), V_{var} are the corresponding detrended daily mean catchment values, $\overline{V_{var}}[m]$ and $\sigma(V_{var}[m])$ are the monthly mean and standard deviation of the variable calculated over 1985-2014 using the detrended values. Again,

the anomalies computation is applied to ERA5-Land and PROJ over 1950-2021 and 1971-2100 respectively. It should be noted that the use of anomalies in the analogue method allows to remove a part of the bias between ERA5-Land and W5E5/PROJ.

Step 5:

In order to find an analogue for a day noted *d*, a multivariate approach is implemented based on the sum of the mean square error (mse) between days available in the high-resolution archive (*HR*) and values form the low-resolution products (*LR)*:

$$Diff[d] = mse(A_T^{HR}, A_T^{LR}[d]) + mse(A_{ET0}^{HR}, A_{ET0}^{LR}[d]) + mse(A_P^{HR}, A_P^{LR}[d]) \quad \text{(Eq. 2)}$$

where *A* are the anomalies computed using Equation 1. The day in the archive that minimises *Diff[d]* is then selected as the analogue. To select an analogue with a meteorological pattern that is seasonally representative of day *d*, the analogue search is restricted to a window defined by a Julian day *d* +/- 45 days.

Step 6:

Some tuning of the previously presented analogue method can be done.

For precipitation, the clearly non-Gaussian distribution of daily values could lead to a suboptimal choice of analogue, causing a dry bias problem (Clemins et al., 2019). To avoid this, the mean catchment values for daily precipitation are first transformed by the following equation:

$$V_{var} = V_{var}^{(1/RRexponent)} \quad \text{(Eq. 3)}$$

with *RRexponent* a value that allows to transform the precipitation distribution. Once the Equation 3 is applied, the V_{var} are replaced in Equation 1.

Even when the variables are standardized by Equation 1, there are still large differences between the variables, leading to more weight for some of the variables in Equation~2. Therefore the Equation 2 is now modified to allow tuning of a weight parameter for precipitation (W_p):

$$Diff[d] = mse(A_T^{HR}, A_T^{LR}[d]) + mse(A_{ET0}^{HR}, A_{ET0}^{LR}[d]) + W_p \times (A_P^{HR}, A_P^{LR}[d]) \quad \text{(Eq. 4)}$$

Finally, when the *Diff[d]* is computed using Equation 2 or Equation 4, instead of selecting only one analogue day, we select the *M* analogue days that minimize the *Diff[d]* values. This allows to create an ensemble of members that can reflect the uncertainty associated with the downscaling step.

Step 7:

The final step consists of adding the linear trends previously removed to the analogue day values.

2.2.2 Creation of the high-resolution climate projections

The downscaling method is applied, using ERA5-Land over the period 1950-2021 as a high-resolution archive and PROJ over the period 1971-2100 as low resolution projections. The tuning parameters are fixed – W_p=1, *RRexponent*=3.5 and *M*=20 – through several experiments over the 1995-2005 period to minimize the bias and retrieve a coherent uncertainy (not shown).

This results in 300 -- 3 SSPs x 5 GCMs x 20 member -- daily climate projections at 0.1° resolution over the 1971-2100 period for each of the six catchments.

2.2.3 Hydrological modeling

The distributed JAMS/J2000 hydrological model (Kralisch and Krause, 2006; Krause, 2002, 2001) is based on the Hydrological Response Units (HRU) -- i.e. the division of the catchment into a large number of small parts where the hydrological response is expected to be similar – and allows information to be obtained at stream segments – called reaches.

The model is process-oriented, taking into account process dynamics at both the reach and HRU level to account for surface, subsurface and groundwater flow from hillslopes into the stream and along stream segments to the outlet.

In addition, JAMS/J2000 simulates plant-related ecohydrological processes as well as the soil water balance and groundwater processes at the HRU level and, based on this, various runoff components at the reach level. JAMS/J2000 was implemented on the 6 case study catchments. The version implemented on 5 catchments - except Guadiaro - also has a snow module to account for snow-related processes.

The calibration of the snow module was done by comparing the snow cover area produced by JAMS/J2000 and MODIS -- a satellite derived product -- (Hall and Riggs, 2020). The calibration used an NSGA II algorithm (Deb et al., 2002) and the Kling Gupta Efficiency (Gupta et al., 2009) as the objective function.

For parameter calibration, the J2000/JAMS discharge simulations were compared with several observed discharge time series available for each catchment (see Report D1.2). Due to the size of the catchments and the number of HRUs, the total number of reaches is specific to each catchment: 4964 for Ain, 1940 for Fekete, 1547 for Guadiaro, 3941 for Krka, 7399 for Morava and 2633 for Vantaanjoki. More details about the implementation of the JAMS/J2000 model over the 6 catchments as well as on the calibration procedure are available on Report D1.2.

2.2.4 Hydrological projections

The J2000/JAMS hydrological model allows the initialization of soil and groundwater reservoirs at the catchment scale. For all runs, the reservoirs are initially set to zero and a 14-year warm-up period is run to properly simulate the internal states of the model.

For all runs, daily variables are extracted at different spatial scales:

- At the reach scale: discharge, contribution from groundwater and soil reservoirs,
- At the catchment scale: precipitation, temperature, evapotranspiration, soil and groundwater reservoirs levels, snow, snow depth, snow melt, actual evapotranspiration.

Firstly, the J2000/JAMS hydrological model is run forced by the ERA5-Land reanalysis over the period 1971-2021. Secondly, the high-resolution projections produced by the downscaling method are also used to force the distributed hydrological model over the 1971-2100 period -- warm up included. The process is repeated for each combination of SSPs x GCMs x number of members and for each of the six case study catchments.

For the sake of simplicity, the hydrological reconstruction obtained using ERA5-Land as forcing will be called ERA5-Land as well while the hydrological projections will be refered by the GCM names used as low resolution information into the downscaling method.

3 Results

3.1 Validation over the 1985-2014 period

The purpose of this section is to validate the hydrological projections obtained for the period 1985-2014 by forcing the JAMS/J2000 model with the climate downscaled projections presented in the previous section. To do this, the hydrological projections obtained are compared with the reconstruction obtained by feeding JAMS/J2000 with the ERA5-Land reanalysis for the corresponding period.

First, the monthly interannual discharges of the two products at the outlet of the 6 catchments are compared in Figure 2:

- For the Ain catchment, the seasonality of the hydrological projections is representative of the one obtained in ERA5-Land hydrological reconstruction. Moreover, the ensemble obtained by using the five GCMs and the 20 analogue days leads to an uncertainty that seems satisfying.
- For Fekete, the seasonality is also well reconstructed, but a strong uncertainty arises from both the five GCMs and the 20 analogue days. Some of the GCMs tend to overestimate the discharge – MPI-ESM1-2-HR for example – while others tend to underestimate the discharge – IPSL-CM6A-LR – over the whole year. All in all, this high uncertainty leads to a reliable ensemble.
- Globally, the discharge at the Guadiaro outlet is accurately reproduced even for the low-flows that occur in summer. However, for November and December an underestimation is visible, probably linked to the underestimation of precipitation over those months (not shown). Concerning the uncertainty, the ensemble seems to be reliable.
- The behaviour of the Krka catchment is also adequately captured, except for the month of December, where all projections seem to underestimate the discharge. This could be related to the underestimation of downscaled precipitation during the months of November and December, about -15% for all climate projections (not shown).

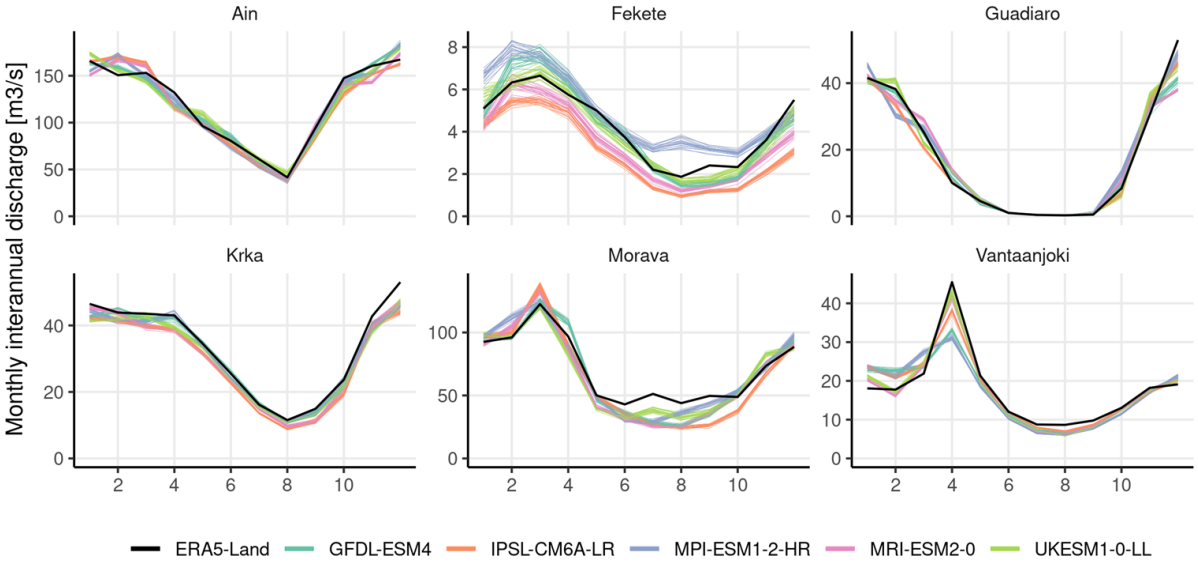

Figure 2: Monthly interannual discharges of JAMS/J2000 forced by ERA5-Land and forced by the downscaled projections at the outlet over the 1985-2014 period.

- For Morava, the hydrological projections correctly reproduced the ERA5-Land hydrological reconstruction for the winter and spring. However, for the summer and autumn months, an underestimation of the discharge is clearly visible in all projections. As for Krka, the cause is to be found in the downscaled climate projections, which suffer from a strong underestimation during the spring and summer seasons, -5 to -10% depending on the projections (not shown).
- In Vantaanjoki, the hydrological projections have difficulties to reproduce the snowmelt maximum that occurs in April. In fact, some of the GCMs – GFDL-ESM4, IPSL-CM6A-LR and MRI-ESM2-0 – overestimate the discharges during the winter months due to an overestimation of temperature during these months (not shown) leading to more liquid precipitation and a deficit in snowpack. At the end of spring, when the temperature rises, the amount of snow storage in the catchment is not sufficient to correctly reproduce the snowmelt. Furthermore, a small underestimation of summer discharge is also visible, probably related to the deficit of precipitation in the climate projection for these months (not shown).

The comparison of the hydrological projections and the hydrological reconstruction from ERA5-Land has shown the quality of these projections for the six catchments, although some weaknesses have been found regarding low flows and annual maxima.

3.2 Analysis of the hydrological projections over the 1985-2100 period

The aim of this section is to provide an overview of the main characteristics of the hydrological projections obtained for the period 1985-2100 in terms of annual and seasonal change and low-flow evolution.

First, the annual and seasonal mean changes for two future periods – 2041-2070 and 2071-2100 – w.r.t 1985-2014 are examined at the outlet of each catchment in Figure 3.

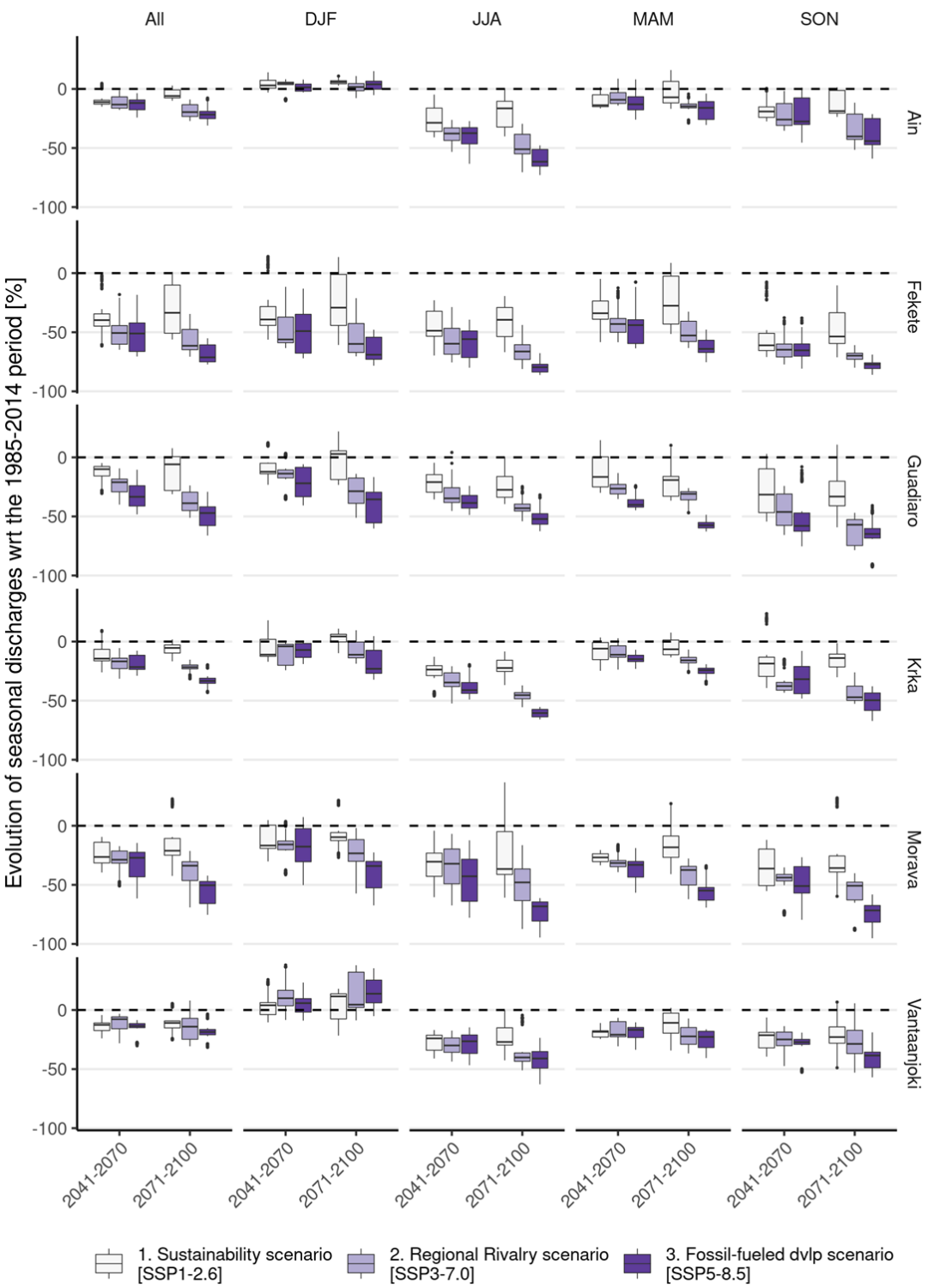

Figure 3: Changes in seasonal mean discharge values at the outlets for 3 thirty-year periods centered in 2035, 2060 and 2085 and the three SSPs. The boxplot represents the uncertainty due to the use of several GCMs.

Future projections show a decrease of annual discharge for all catchments – except for Vantaanjoki – regardless of the SSP and the future periods considered. For SSP1-2.6, the decrease is more important over the mid-century period [2041-2070] than the end of the century [2071-2100] showing a relative recovering due to a climate closer to the historical one at the end of the century. In contrary, for SSP3-7.0, the decrease is stronger at the end of the century and significatively more intense than the one observes with SSP1-2.6. The SSP5-8.5 shows a similar evolution with an even more pronounced decrease of the annual discharge.

During the winter months - December, January and February - there is a small increase for Ain and a more pronounced one for Vantaanjoki. For these two catchments, the difference between SSPs does not appear to be significant and the magnitude of change does not evolve through the different periods. For Fekete, Guadiaro, Krka and Morava, the winter months become drier in the future – in particular at the end of the century – and the magnitude of change is strongly linked to the SSPs, i.e. a larger change with SSP5-8.5 than SSP3-7.0 and than SSP1-2.6.

For all other seasons - spring, summer and autumn - we observe a decrease of discharge for all catchments, regardless of the SSP or the time period considered. However, the magnitude of the decrease is not the same for each catchment. Overall, the magnitude of the decrease depends on the time period - higher decrease in the far future - and the SSP - higher decrease for SSP3-7.0 and especially for SSP5-8.5.

In order to better recognize the role of each of the driving factors, an ANOVA is performed on the mean discharge at the outlet for the months of June, July and August, and is presented in Figure 4.

Overall, in the historical period the GCMs are the main factor explaining the summer discharge and the selection of 20 member analog days – designed by Downscaling in the legend – does not appear to be a relevant part of the uncertainy, execpted for Guadiaro. During the historical period, the part of variance explained by the SSPs are equal to zero because the emission scenario are the same for each SSP.

For the near future, the main source of uncertainty comes from the different GCMs used as input in the downscaling method, except for Vantannjoki where the uncertainty is dominated by the residuals. This could means that natural variability is the first factor explaining the uncertainty in Vantaanjoki's discharge projections.

Finally, at the end of the century, the SSPs become the first factor explaining the variance, ahead of the GCMs. This is not the case for Vantaanjoki, where the variance is mainly explained by the GCMs, followed closely by the SSPs.

Figure 4: Part of the variance explained in the discharge projections changes of JJA at the outlet for different periods

We lastly focus on the evolution of the 1st decile of discharge over each reach of the DRNs.

The aim is to demonstrate the added value of the distributed hydrological projections through an example. Here only the SSP3-7.0 is considered and the evolution is calculated for the period 2070-2100. Figure 5 shows that for all six sub-catchments the 1st decile is decreasing. The evolution can reach up to -80% with respect to the catchment considered. Furthermore, the distribution of changes is not the same within a sub-catchment. For example, in Lepsämänjoki the decrease is from -80% to -60%, while in other areas it is only from -20% to 0%. Finally, some of the results can be difficult to interpret, for example in the Guadiaro catchment the decrease in summer discharge is about -50% – see Figure 3 – but the 1st decile decreases "only" about -40% to -20%, while in the Ain catchment the decrease in summer discharge is also close to -50% – see Figure 3 – and leads to a decrease of -100% to -80% for a large part of the catchment. This is probably due to the fact that the Guadiaro catchment is already a very dry catchment during the summer season with 1st decile value equal to zero for some reaches even in the historical period.

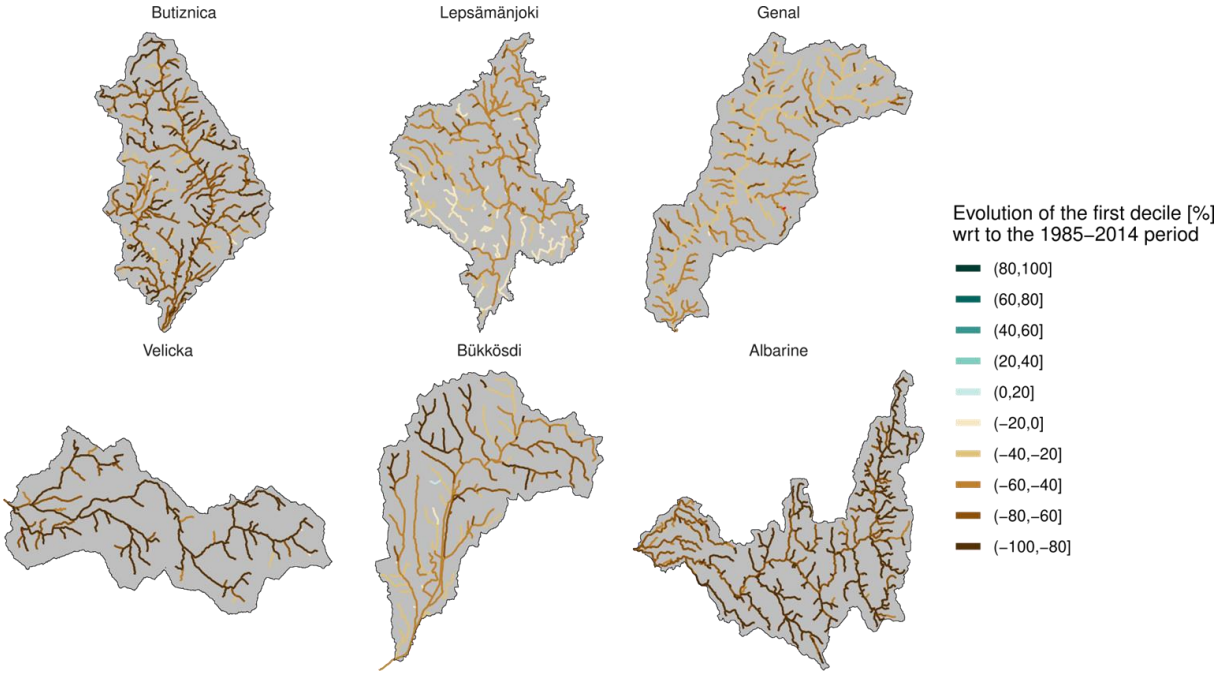

Figure 5: Evolution of the 1st decile of discharge over the DRNs for the SSP3-7.0 and the 2070-2100 period. Maps show the mean of the 5 GCMs x 20 members.

4 Conclusions

The present study provides distributed daily reach-scale hydrological projections for six European catchments for the period 1985-2100.

To obtain these projections, a multivariate downscaling method based on the analogue approach has been applied to diverse coarse climate projections from ISIMIP. This involves the use of five different GCMs forced by three different SSPs as predictand to resample the high-resolution ERA5-Land reanalysis using daily mean catchment precipitation, evapotranspiration and temperature. The analogue method led to the generation of daily high-resolution climate projections -- 0.1°, i.e. similar to ERA5-Land -- which have been used to force the JAMS/J2000 distributed hydrological model. The combination allows to obtain reach-scale daily discharge, groundwater and soil contribution, but also other variables aggregated at the catchment scale.

A focus was made on the validation of hydrological projections over the historical period 1985-2014. Globally, the projections correctly reproduced the monthly seasonal cycle at the outlet. However, some discrepancies also appear for summer discharge in the Morava and Vantaanjoki catchments, showing a relatively dry bias for these months. Finally, for the Vantaanjoki catchment, some of the GCMs produced a winter that was too warm compared to ERA5-Land, leading to an underestimation of the snow cover and thus of the snowmelt-related peak discharge in April. The comparison also showed that the use of the five GCMs and the 20 members of the analogue approach resulted in sufficient dispersion to produce a reliable ensemble, except for the bias mentioned above.

For the hydrological projections, an analysis was carried out to summarise some of the changes for three different time periods – 2041-2070 / 2071-2100 – with respect to 1985-2014. The responses of the six catchments were clearly different, showing an impact of climate change closely related to their

location. For discharge, spring, summer and autumn show a decrease for all catchments and all SSPs considered. For winter discharge, two of the catchments show a slight increase, but the other four also show a decrease. Overall, the projections also agree for a decrease in the annual discharge.

Finally, an analysis focusing on the change in low flows has also put forward the interest of distributed discharge as the change is not exactly the same in each part of the catchment considered.

In order to better analyse the impact of the GCM, SSP and the downscaling ensemble due to the analogue approach, a decomposition of the variance over the summer season has been carried out. For the hydrological projections, the decomposition has shown the strong influence of the GCMs on the uncertainty for the near future period and, conversely, a stronger influence of the SSPs for more distant futures, indicating drastic differences between these scenarios.

Given the results, the hydrological projections will be used in a forthcoming study to derive flow condition projections for the six DRNs using a Random Forest algorithm and the results will be used in the DRYvER project to model the evolution of the meta-communities on diverse intermittent rivers.

5 References

Allen, R.G., Pereira, L.S., Raes, D., Smith, M., n.d. Crop evapotranspiration - Guidelines for computing crop water requirements - FAO Irrigation and drainage paper 56.

Arias, P., Bellouin, N., Coppola, E., Jones, R., Krinner, G., Marotzke, J., Naik, V., Palmer, M., Plattner, G.-K., Rogelj, J., Rojas, M., Sillmann, J., Storelvmo, T., Thorne, P., Trewin, B., Achutarao, K., Adhikary, B., Allan, R., Armour, K., Bala, G., Barimalala, R., Berger, Sophie, Canadell, J.G., Cassou, C., Cherchi, A., Collins, W.D., Collins, W.J., Connors, S., Corti, S., Cruz, F., Dentener, F.J., Dereczynski, C., Di Luca, A., Diongue Niang, A., Doblas-Reyes, P., Dosio, A., Douville, H., Engelbrecht, F., Eyring, V., Fischer, E.M., Forster, P., Fox-Kemper, B., Fuglestvedt, J., Fyfe, J., Gillett, N., Goldfarb, L., Gorodetskaya, I., Gutierrez, J.M., Hamdi, R., Hawkins, E., Hewitt, H., Hope, P., Islam, A.S., Jones, C., Kaufmann, D., Kopp, R., Kosaka, Y., Kossin, J., Krakovska, S., Li, J., Lee, J.-Y., Masson-Delmotte, V., Mauritsen, T., Maycock, T., Meinshausen, M., Min, S., Ngo Duc, T., Otto, F., Pinto, I., Pirani, A., Raghavan, K., Ranasighe, R., Ruane, A., Ruiz, L., Sallée, J.-B., Samset, B.H., Sathyendranath, S., Monteiro, P.S., Seneviratne, S.I., Sörensson, A.A., Szopa, S., Takayabu, I., Treguier, A.-M., van den Hurk, B., Vautard, R., Von Schuckmann, K., Zaehle, S., Zhang, X., Zickfeld, K., 2021. Climate Change 2021: The Physical Science Basis. Contribution of Working Group I to the Sixth Assessment Report of the Intergovernmental Panel on Climate Change; Technical Summary, in: Masson-Delmotte, V., Zhai, P., Pirani, A., Conners, S.L., Péan, C., Berger, S., Caud, N., Chen, Y., Goldfarb, L., Gomis, M.I., Huang, M., Leitzell, K., Lonnoy, E., Matthews, J.B.R., Maycock, T.K., Waterfield, T., Yelekçi, O., Yu, R., Zhou, B. (Eds.), . Presented at the The Intergovernmental Panel on Climate Change AR6, Remote.

Clemins, P.J., Bucini, G., Winter, J.M., Beckage, B., Towler, E., Betts, A., Cummings, R., Queiroz, H.C., 2019. An Analog Approach for Weather Estimation Using Climate Projections and Reanalysis Data. J. Appl. Meteorol. Climatol. 58, 1763–1777. https://doi.org/10.1175/JAMC-D-18-0255.1

Copernicus Climate Change Service (C3S) Climate Data Store (CDS), 2023. Copernicus Climate Change Service (C3S) (2022): ERA5-Land hourly data from 1950 to present. https://doi.org/10.24381/cds.e2161bac

Cucchi, M., Weedon, G.P., Amici, A., Bellouin, N., Lange, S., Müller Schmied, H., Hersbach, H., Buontempo, C., 2020. WFDE5: bias-adjusted ERA5 reanalysis data for impact studies. Earth Syst. Sci. Data 12, 2097–2120. https://doi.org/10.5194/essd-12-2097-2020

Datry, T., Allen, D., Argelich, R., Barquin, J., Bonada, N., Boulton, A., Branger, F., Cai, Y., Cañedo-Argüelles, M., Cid, N., Csabai, Z., Dallimer, M., de Araújo, J.C., Declerck, S., Dekker, T., Döll, P., Encalada, A., Forcellini, M., Foulquier, A., Heino, J., Jabot, F., Keszler, P., Kopperoinen, L., Kralisch, S., Künne, A., Lamouroux, N., Lauvernet, C., Lehtoranta, V., Loskotová, B., Marcé, R., Martin Ortega, J., Matauschek, C., Miliša, M., Mogyorósi, S., Moya, N., Müller Schmied, H., Munné, A., Munoz, F., Mykrä, H., Pal, I., Paloniemi, R., Pařil, P., Pengal, P., Pernecker, B., Polášek, M., Rezende, C., Sabater, S., Sarremejane, R., Schmidt, G., Senerpont Domis, L., Singer, G., Suárez, E., Talluto, M., Teurlincx, S., Trautmann, T., Truchy, A., Tyllianakis, E., Väisänen, S., Varumo, L., Vidal, J.-P., Vilmi, A., Vinyoles, D., 2021. Securing Biodiversity, Functional Integrity, and Ecosystem Services in Drying River Networks (DRYvER). Res. Ideas Outcomes 7, e77750. https://doi.org/10.3897/rio.7.e77750

Deb, K., Pratap, A., Agarwal, S., Meyarivan, T., 2002. A fast and elitist multiobjective genetic algorithm: NSGA-II. IEEE Trans. Evol. Comput. 6, 182–197. https://doi.org/10.1109/4235.996017

Eyring, V., Bony, S., Meehl, G.A., Senior, C.A., Stevens, B., Stouffer, R.J., Taylor, K.E., 2016. Overview of the Coupled Model Intercomparison Project Phase 6 (CMIP6) experimental design and organization. Geosci. Model Dev. 9, 1937–1958. https://doi.org/10.5194/gmd-9-1937-2016

Frieler, K., Volkholz, J., Lange, S., Schewe, J., Mengel, M., Rivas López, M. del R., Otto, C., Reyer, C.P.O., Karger, D.N., Malle, J.T., Treu, S., Menz, C., Blanchard, J.L., Harrison, C.S., Petrik, C.M., Eddy, T.D., Ortega-Cisneros, K., Novaglio, C., Rousseau, Y., Watson, R.A., Stock, C., Liu, X., Heneghan,

R., Tittensor, D., Maury, O., Büchner, M., Vogt, T., Wang, T., Sun, F., Sauer, I.J., Koch, J., Vanderkelen, I., Jägermeyr, J., Müller, C., Klar, J., Vega del Valle, I.D., Lasslop, G., Chadburn, S., Burke, E., Gallego-Sala, A., Smith, N., Chang, J., Hantson, S., Burton, C., Gädeke, A., Li, F., Gosling, S.N., Müller Schmied, H., Hattermann, F., Wang, J., Yao, F., Hickler, T., Marcé, R., Pierson, D., Thiery, W., Mercado-Bettín, D., Forrest, M., Bechtold, M., 2023. Scenario set-up and forcing data for impact model evaluation and impact attribution within the third round of the Inter-Sectoral Model Intercomparison Project (ISIMIP3a). EGUsphere 1–83. https://doi.org/10.5194/egusphere-2023-281

Gupta, H.V., Kling, H., Yilmaz, K.K., Martinez, G.F., 2009. Decomposition of the mean squared error and NSE performance criteria: Implications for improving hydrological modelling. J. Hydrol. 377, 80–91. https://doi.org/10.1016/j.jhydrol.2009.08.003

Hall, D.K., Riggs, G.A., 2020. MODIS/Terra Snow Cover 8-Day L3 Global 500m SIN Grid, Version 61 [Data Set]. https://doi.org//10.5067/MODIS/MOD10A2.061

Harris, I., Osborn, T.J., Jones, P., Lister, D., 2020. Version 4 of the CRU TS monthly high-resolution gridded multivariate climate dataset. Sci. Data 7, 109. https://doi.org/10.1038/s41597-020-0453-3

Hersbach, H., Bell, B., Berrisford, P., Hirahara, S., Horányi, A., Muñoz-Sabater, J., Nicolas, J., Peubey, C., Radu, R., Schepers, D., Simmons, A., Soci, C., Abdalla, S., Abellan, X., Balsamo, G., Bechtold, P., Biavati, G., Bidlot, J., Bonavita, M., De Chiara, G., Dahlgren, P., Dee, D., Diamantakis, M., Dragani, R., Flemming, J., Forbes, R., Fuentes, M., Geer, A., Haimberger, L., Healy, S., Hogan, R.J., Hólm, E., Janisková, M., Keeley, S., Laloyaux, P., Lopez, P., Lupu, C., Radnoti, G., de Rosnay, P., Rozum, I., Vamborg, F., Villaume, S., Thépaut, J.-N., 2020. The ERA5 global reanalysis. Q. J. R. Meteorol. Soc. 146, 1999–2049. https://doi.org/10.1002/qj.3803

Iman, R.L., 2014. Latin Hypercube Sampling, in: Wiley StatsRef: Statistics Reference Online. John Wiley & Sons, Ltd. https://doi.org/10.1002/9781118445112.stat03803

Kralisch, S., Krause, P., 2006. JAMS – A Framework for Natural Resource Model Development and Application. Presented at the iEMSs Third Biannual Meeting.

Krause, P., 2002. Quantifying the impact of land use changes on the water balance of large catchments using the J2000 model. Phys. Chem. Earth Parts ABC 27, 663–673. https://doi.org/10.1016/S1474-7065(02)00051-7

Krause, P., 2001. Das hydrologische Modellsystem J2000 - Beschreibung und Anwendung in großen Flußgebieten, Schriften des Forschungszentrums Jülich. Reihe Umwelt / Environment. Forschungszentrum Jülich GmbH Zentralbibliothek, Verlag, Jülich.

Lange, S., 2019a. WFDE5 over land merged with ERA5 over the ocean (W5E5). https://doi.org/10.5880/PIK.2019.023

Lange, S., 2019b. Trend-preserving bias adjustment and statistical downscaling with ISIMIP3BASD (v1.0). Geosci. Model Dev. 12, 3055–3070. https://doi.org/10.5194/gmd-12-3055-2019

Lorenz, K.Z., 1974. Analogy as a Source of Knowledge. Science 185, 229–234. https://doi.org/10.1126/science.185.4147.229

Messager, M.L., Lehner, B., Cockburn, C., Lamouroux, N., Pella, H., Snelder, T., Tockner, K., Trautmann, T., Watt, C., Datry, T., 2021. Global prevalence of non-perennial rivers and streams. Nature 594, 391–397. https://doi.org/10.1038/s41586-021-03565-5

Muñoz-Sabater, J., Dutra, E., Agustí-Panareda, A., Albergel, C., Arduini, G., Balsamo, G., Boussetta, S., Choulga, M., Harrigan, S., Hersbach, H., Martens, B., Miralles, D.G., Piles, M., Rodríguez-Fernández, N.J., Zsoter, E., Buontempo, C., Thépaut, J.-N., 2021. ERA5-Land: a state-of-the-art global reanalysis dataset for land applications. Earth Syst. Sci. Data 13, 4349–4383. https://doi.org/10.5194/essd-13-4349-2021

Schneider, U., Becker, A., Finger, P., Rustemeier, E., Ziese, M., 2020. GPCC Full Data Monthly Product Version 2020 at 0.25°: Monthly Land-Surface Precipitation from Rain-Gauges built on GTS-based and Historical Data. https://doi.org/10.5676/DWD_GPCC/FD_M_V2020_025

Shiogama, H., Ishizaki, N.N., Hanasaki, N., Takahashi, K., Emori, S., Ito, R., Nakaegawa, T., Takayabu, I., Hijioka, Y., Takayabu, Y.N., Shibuya, R., 2021. Selecting CMIP6-Based Future Climate Scenarios for Impact and Adaptation Studies. Sola 17, 57–62. https://doi.org/10.2151/sola.2021-009

6 Supplementary Material

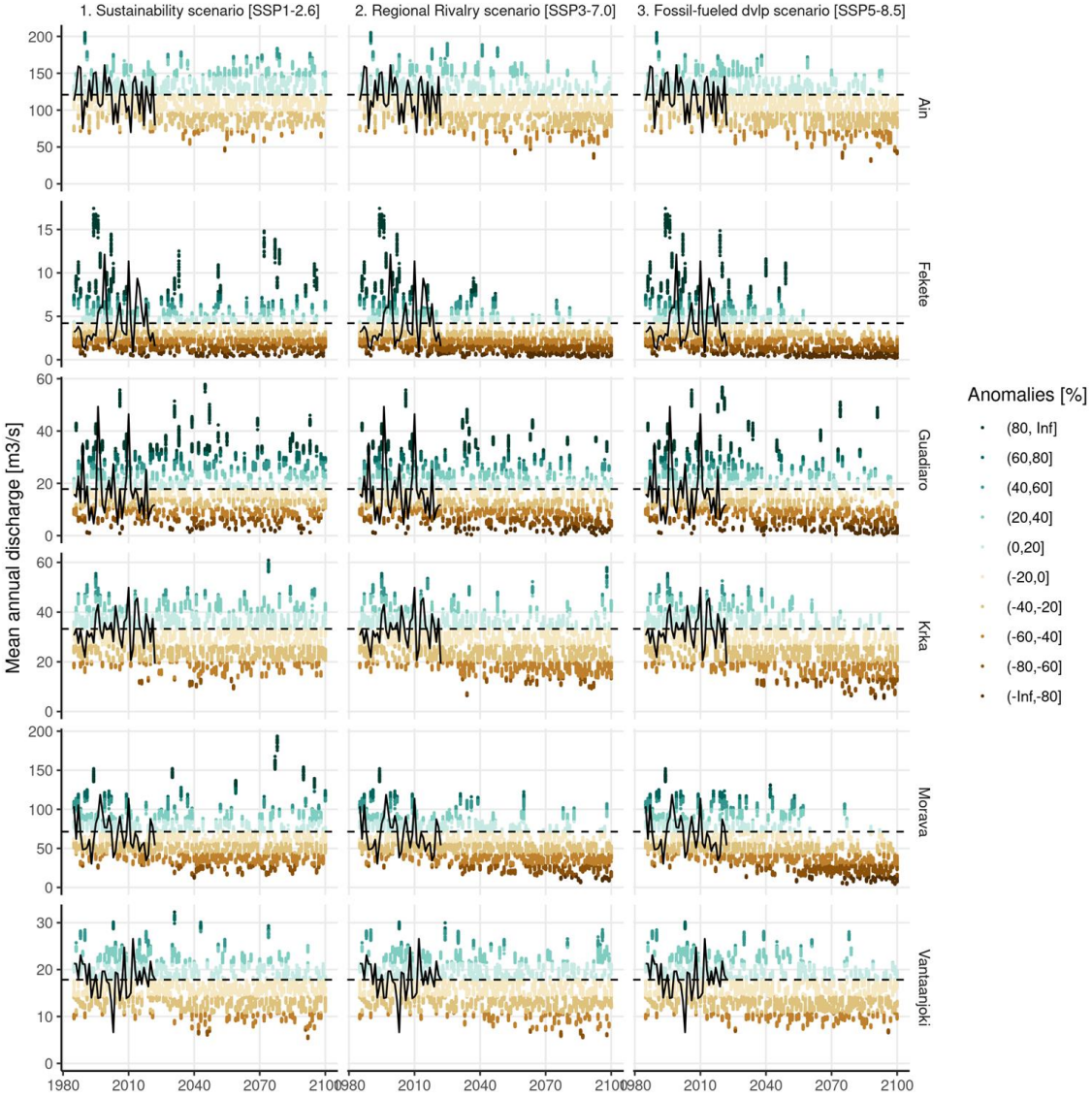

Figure 6: Evolution of mean annual discharge for all hydrological projections. The anomalies are given w.r.t the 1985-2014 period.